Fiber Bragg Grating Sensors-Based Thermometry of Gold Nanorod-Enhanced Photothermal Therapy in Tumor Model

Leonardo Bianchi, *Graduate Student Member, IEEE*, Rachael Mooney, Yvonne Cornejo, Caitlyn Hyde, Emiliano Schena, *Senior Member, IEEE*, Jacob M. Berlin, Karen Aboody, and Paola Saccomandi, *Senior Member, IEEE*

***Abstract*—This work proposes the use of femtosecond laser-written fiber Bragg grating (FBG) sensors for internal temperature monitoring of tumors undergoing gold nanorod (AuNR)-mediated photothermal therapy (PTT). Arrays of sub-millimetric FBGs enabled an accurate and quasi-distributed temperature measurement within subcutaneous breast tumors in mice. Furthermore, FBGs permitted to investigate the laser-tissue interaction and AuNR-assisted photothermal enhancement on cancerous tissue exposed to 940 nm and 1064 nm radiations. The introduction of the tumor-localized AuNRs resulted in an overall increase of 13 °C of the mean temperature change, compared to control, in case of 1064 nm, while ∼6 °C in case of 940 nm. This sensing solution allows the minimally invasive measurement of the internal tumor temperature under AuNR-assisted PTT. This feasibility study sets the basis for the evaluation of the thermal outcome mediated by nanoparticles under different laser sources.**

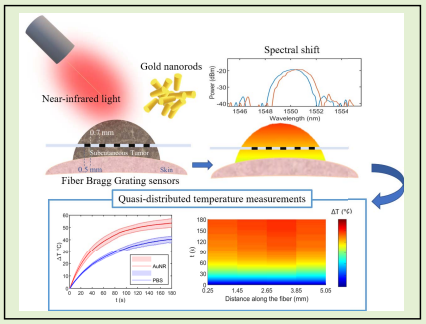

***Index Terms*— Fiber Bragg grating sensors, temperature sensors, femtosecond laser inscription, temperature measurement, gold nanorods, photothermal therapy, laser.**

Manuscript received March 1, 2021; revised May 8, 2021; accepted May 17, 2021. This work was supported by the European Research Council (ERC) through the European Union's Horizon 2020 Research and Innovation Programme under Grant 759159. The work of Emiliano Schena was supported in part by the Outgoing Visiting Programme-Spring Term 2019 of the Università Campus Bio-Medico di Roma. The associate editor coordinating the review of this article and approving it for publication was Prof. Gijs J. M. Krijnen. *(Corresponding author: Paola Saccomandi.)*

This work involved animals in its research. Approval of all ethical and experimental procedures and protocols was granted by the City of Hope Beckman Research Institute Institutional Animal Care and Use Committee.

Leonardo Bianchi and Paola Saccomandi are with the Department of Mechanical Engineering, Politecnico di Milano, 20156 Milan, Italy (e-mail: leonardo.bianchi@polimi.it; paola.saccomandi@polimi.it).

Rachael Mooney, Caitlyn Hyde, and Karen Aboody are with the Department of Developmental and Stem Cell Biology, Beckman Research Institute of City of Hope, Duarte, CA 91010 USA (e-mail: rmooney@coh.org; chyde@coh.org; kaboody@coh.org).

Yvonne Cornejo was with the Department of Developmental and Stem Cell Biology, Beckman Research Institute of City of Hope, Duarte, CA 91010 USA. She is now with the Laboratory Animal Veterinarian at Valley Biosystems, West Sacramento, CA 95605 USA (e-mail: ycornejo235@gmail.com).

Emiliano Schena is with the School of Engineering, Università Campus Bio-medico di Roma, 00128 Rome, Italy (e-mail: e.schena@unicampus.it).

Jacob M. Berlin was with Beckman Research Institute of City of Hope, Duarte, CA 91010 USA. He is now with Terray Therapeutics, Pasadena, CA 91106, USA (e-mail: jacobberlincoh@gmail.com).

Digital Object Identifier 10.1109/JSEN.2021.3082042

I. Introduction

MANY more people in Europe are living with cancer as the result of an aging population, unhealthy lifestyles, and unfavorable working and environmental conditions. Among all, breast cancer is the second cause of cancer death in women, despite the decreasing mortality trends since the nineties. However, due to the aging of the population, the absolute number of deaths is stable and above 92000 [1]. Thus, the medical and public health burden of breast cancer in Europe is not expected to decrease, and effective diagnostic and therapeutic approaches are constantly demanded. To raise consciousness on this matter, also the Horizon Europe Framework Programme for Research and Innovation (2021-2027) has designed a specific Mission on Cancer [2]. This mission includes several actions, including the need of optimizing treatment, with the goal of averting more than 3 million additional premature deaths due to cancer by 2030. Besides the traditional approaches for breast cancer, photothermal therapy (PTT) is attracting increasing attention as a potential alternative therapy, thanks to its minimally invasive nature [3], [4]. Here, light irradiation, delivered as an external stimulus, is converted to heat by agents in the nanoscale format [5], [6]. The interaction between light and nanoparticles leads to the temperature increase of the target

tissue while preserving the healthy regions around. In the PTT application, rod-shaped gold nanoparticles, i.e., gold nanorods (AuNRs), have been largely investigated since they can strongly absorb electromagnetic waves at different wavelengths in the near-infrared (NIR) range, which is favorable for the penetration of the light into the tissue. Moreover, AuNRs have shown high heating efficiency, which is crucial to assure therapy selectivity. As expected, tissue temperature is the key parameter to assure the PTT efficacy and safety. Indeed, it has been proven that temperatures ranging from 55 °C to 95 °C are needed to generate tumorigenic damage in *in vivo* conditions [7].

Whereas important scientific and technological efforts have been made in the last 2 decades for the design and synthesis of optimized nanoparticles for PTT, less attention has been paid to the approaches for accurately monitoring the thermal outcome during the treatments. Although light-absorbing nanoparticles injected in tumors determine the localized increase of tissue temperature, several factors, such as particles concentration and distribution and light source settings can affect the thermal outcome, including temperature distribution and tumorigenic damage [5].

Temperature measurement can provide useful information to design the optimal therapy settings, and the real-time monitoring will further support the clinician by providing feedback to adjust therapy in real-time. Especially in pre-clinical tests for preoperative optimization of PTT settings, the characteristics of the sensing methods are crucial for accurate detection of temperature profiles in treated tumors. For instance, thermocouples [8], [9] suffer from self-heating and single-point measurements [4], thus presenting several limitations for optimal temperature monitoring. Image-based techniques, such as infrared thermography and Magnetic Resonance Thermal Imaging (MRTI), hold the benefit of providing information on the temperature distribution. The second approach is very promising but suffers from limited availability in most of the research laboratories. Moreover, a few studies have reported the use of MRTI for AuNR-mediated PTT and mostly in agar-gel phantom [10]. This may be due to the low performance of gold alone as a contrast agent, thus, the interest in exploring MRTI is addressed mostly towards the use of magnetic or gadolinium-based nanoparticles with MRI contrast-enhancing capabilities [6], [11].

A good compromise between the straightforward use of sensors and the need for spatially distributed temperature measurements can be offered by fiber optic sensors (FOSs). According to the specific technology, FOSs offer the possibility to achieve distributed and quasi-distributed sensing along the axis of the fiber [12]. The first technology enables paramount features for spatially resolved thermometry, i.e., hundreds of simultaneous measurements in one optical fiber with millimetric resolution; however, it is usually impaired by the trade-off between the desired spatial resolution, the signal quality, and the time resolution. Conversely, quasi-distributed sensing based on Fiber Bragg Grating (FBG) technology can achieve tens of measurement points with high signal-to-noise ratio [13], [14]. The recent writing technology based on the femtosecond laser inscription allows for sub-millimetric sensor length with reflectivity suitable for the peak-tracking techniques implemented by most interrogators [15]. This technique allows also customizing the gratings and array features, thus improving its capability to multiplex sensor outputs [16].

FBGs with sub-millimetric sensing length can be fabricated in high temperature resistant polyimide-coated fibers, in order to be suitable for thermometry during minimally invasive thermal therapies for tumors [13], [17]–[19], [20]–[23], such as PTT [24]. In addition, FBGs particularly fit biomedical applications, due to their biological and chemical inertness, lightweight and compact form factor, biocompatibility, and fast time response [19].

For the mentioned reasons, FBG arrays can represent a valid solution for detecting the effective temperature increase due to the tumor-embedded nanoparticles.

In this work, we investigate the feasibility of using FBGs arrays for monitoring the internal tumor temperature change caused by AuNRs. To the best of our knowledge, this is the first study applying FBG arrays for real-time thermometry in animal tumor models undergoing AuNRs-mediated PTT. The arrays written in the core of polyimide-coated fibers consist of 5 FBGs, which have been customized in order to achieve a 0.5 mm sensing length. The sensors have been characterized in terms of static and dynamic metrological characteristics, and an evaluation of the potential breathing-induced strain influence has been carried out. AuNRs-mediated PTT was executed at two different NIR wavelengths (940 nm and 1064 nm) in subcutaneous breast tumor-bearing mice, and the thermal analysis was performed with the customized sub-millimetric FBGs arrays located into the tumors.

II. Fiber Optic-Based Sensing

In the following sections, the working principle of the employed FOSs and their static and dynamic calibrations are reported.

A. Fiber Bragg Grating Sensors: Working Principle

FBGs consist of photo-inscribed microstructures within the fiber core, characterized by periodical modifications of the core refractive index. These sensors act as selective wavelength reflectors due to their capability, once interrogated by means of broadband light, to reflect a narrowband part of the spectrum centered at the so-called Bragg wavelength, λ_B. This wavelength is directly proportional to the effective refractive index n_{eff} and the spatial grating period Λ, i.e., the distance between two regions characterized by high values of refractive index [25], (1):

$$\lambda_B = 2 \cdot n_{eff} \cdot \Lambda \tag{1}$$

Temperature variations (ΔT) and mechanical strains (ε) cause a change of $\lambda_B(\Delta\lambda_B)$, according to the following equation [26]:

$$\frac{\Delta\lambda_B}{\lambda_B} = P_e \cdot \varepsilon + [P_e \cdot (\alpha_{cl} - \alpha_{co}) + \xi] \cdot \Delta T \tag{2}$$

where P_e represents the strain-optic coefficient, α_{cl} and α_{co} are the thermal expansion coefficients of the fiber bonding

material, i.e., the cladding material, and of the inner core, respectively, and ξ is thermo-optic coefficient of the optical fiber. In case of negligible strain, the alteration of λ_B is dependent only upon temperature perturbations according to the change of the period of index modulation, due to the material thermal expansion, and variations of n_{eff}. Therefore, (2) can be simplified and expressed as:

$$\frac{\Delta\lambda_B}{\lambda_B} = S_t \cdot \Delta T \tag{3}$$

being S_t the thermal sensitivity of the grating.

Multipoint temperature measurements across a single fiber can be achieved by embedding different gratings, characterized by different nominal λ_B, in the fiber itself. The resulting FBG array allows for quasi-distributed sensing, hence the possibility to obtain discrete temperature profiles.

In the present study, custom-made arrays of 5 FBGs were adopted (FiSens GmbH, Braunschweig, Germany). Femtosecond point-by-point writing technology was exploited in order to inscribe FBG arrays in the core of a single-mode optical fiber (1550 nm wavelength operation range, 10 nm distance between Bragg wavelengths of consecutive gratings, polyimide-coated fiber with a diameter of ~150 μm).

This technique allows inscribing gratings with high precision in materials that are not photosensitive and to customize the grating characteristics to attain a vast range of grating lengths [16]. Moreover, FBGs attained with femtosecond lasers are characterized by high thermal stability in comparison to UV light-induced FBGs [27], and display high reflectivity when inscribed in resistant protective coating (e.g., polyimide coating) [28]. All these features make femtosecond laser-induced gratings well suited for temperature monitoring of laser thermotherapies. In particular, the selection of the protective coating material utilized in this study refers to the high performances, the high mechanical strength, and peculiar thermal properties of polyimide, e.g., low thermal conductivity [12], [29], and high-temperature resistance, when compared to the standard acrylate coatings [16]. These characteristics may be beneficial for thermal monitoring of nanoparticle-mediated photothermal and laser-assisted therapies where high temperatures (>100 °C) can be observed [30].

The total sensing length of the array was designed to fit the typical diameter of a subcutaneous tumor in mice (~5 mm -7 mm [31]), thus the grating length (i.e., 0.5 mm) and edge-to-edge distance between gratings (i.e., 0.7 mm) were chosen consequently. The discrimination of the FBGs in the portion of the spectrum ranging from 1460 nm to 1620 nm of the Micron Optics HYPERION si255 optical sensing interrogator (Micron Optics, Atlanta, USA, wavelength accuracy 1 pm, corresponding to 0.1 °C), thus the wavelength-division multiplexing of the FBGs, was assured by the change of grating periods along the array, performed while inscribing the fiber. The optical reflected spectrum of the FBG array measured by the optical spectrum analyzer is displayed in Fig. 1 (the FBG sensors were characterized by a reflectivity value >30%).

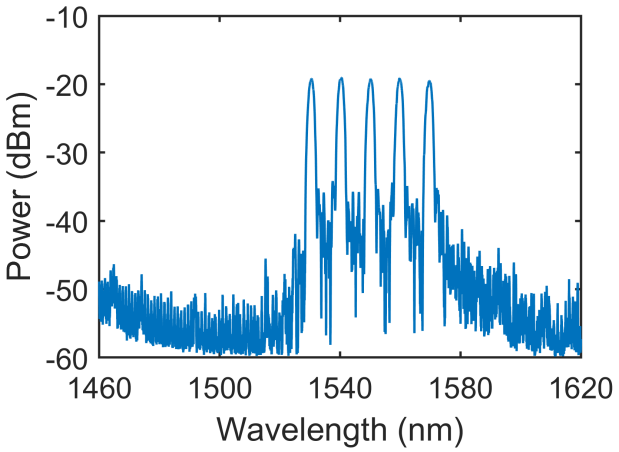

Fig. 1. Reflection spectrum of the FBG array fabricated with femtosecond point-by-point writing technology: 5 peak Bragg reflections equidistant in the 1530.6 nm - 1569.7 nm wavelength range.

B. Static and Dynamic Calibrations

The sensors response to a temperature variation of about 100 °C was evaluated to assess the S_t. Particularly, FBG sensors were calibrated in a thermostatic chamber in the temperature range from 27 °C to 130 °C. The selected temperature interval was chosen to ensure to include the temperature values to which the sensors were subjected during the experimental procedures. The tests were repeated three times.

Concerning the dynamic response of the FBG sensors, the response time τ was evaluated by transferring the segment of the optical fiber embedding the array of 5 FBG sensors from room temperature to a vessel filled with warm water, at a temperature of about 36 °C, that was monitored by a type K thermocouple (0.1 °C accuracy). The described experimental procedure was repeated three times.

The optical reflected spectrum of the FBG array was measured by the spectrum analyzer (sample frequency of 1 kHz, which is the highest selectable value). Considering a first-order system as a model of the sensor response [32], the value of τ was estimated through the linear regression of the natural logarithm of the error fraction function $\Gamma(t)$:

$$\Gamma(t) = \frac{y(t) - y_{ss}}{y_0 - y_{ss}} = e^{-\frac{t}{\tau}} \tag{4}$$

being $y(t)$ the output value at the instant t, y_0 the value at the beginning of the step, and y_{ss} the output value at the steady state.

III. Photothermal Treatment

The following paragraphs describe the establishment of the tumor model, the subsequent administration of the laser-absorbing AuNRs, the experimental setup to perform the photothermal procedure, and the related FBG-based temperature monitoring.

A. Tumor Model and AuNRs Injection

The City of Hope Beckman Research Institute Institutional Animal Care and Use Committee reviewed and approved

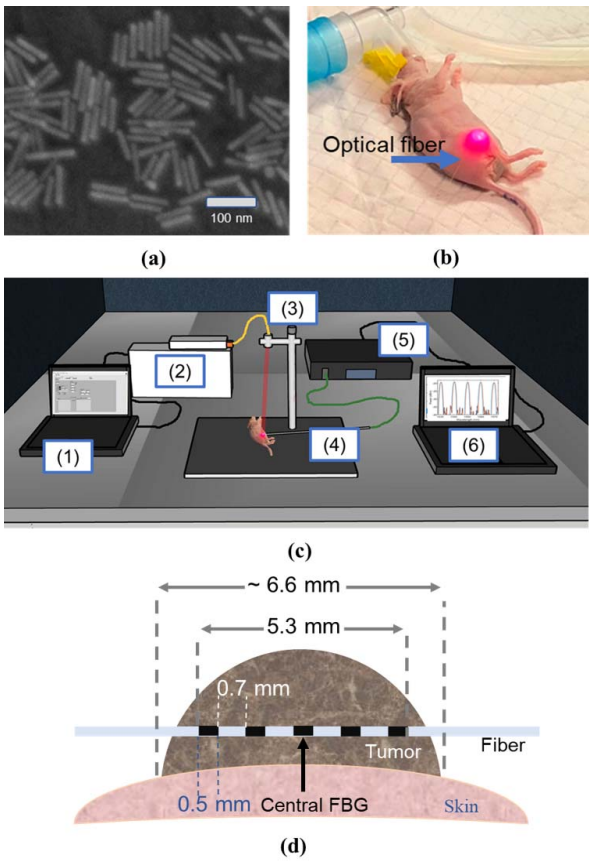

Fig. 2. (a) Scanning electron microscope image of MUTAB-coated AuNRs. (b) Image of a tumor-bearing mouse with the optical fiber used for quasi-distributed temperature measurements. (c) Experimental set-up: (1) laser settings control system, (2) laser source module, (3) laser tip, (4) optical fiber, (5) interrogation unit, (6) system employed for the spectral analysis. (d) Position of fiber embedding the array of 5 FBGs inside the tumor.

all the animal procedures. Athymic nude mice (Charles River) were injected in upper thigh with 10,000 Red firefly luciferase (Red-FLuc) 4T1 breast cancer cells in 50 μL RPMI and 50 μL Matrigel. Sixteen days after tumors establishment, a charge-coupled device camera (Xenogen IVIS-100, Xenogen Corporation, Almeda, CA) was used to confirm viable engraftment. Tumors were divided into four treatment groups (3 tumors/group). The first two groups were selected to undergo laser irradiation at a wavelength of 940 nm. Therefore, the first group was injected with 11-mercaptoundecyltrimethylammonnium bromide (MUTAB)-coated AuNRs, provided by Nanopartz™, with peak absorption at 950 nm to match with the corresponding radiation wavelength; the second group was injected with saline solution (Phosphate-buffered saline, PBS) to evaluate the thermal tumor response in absence of the nanoparticles. The third and fourth groups were chosen to be exposed to 1064 nm-radiation, and they were respectively injected with MUTAB-coated AuNRs (peak absorption at 1050 nm, Nanopartz™) and PBS. The amount of AuNRs for each tumor injection was 12.5 μg, while the injected volume of PBS was 20 μL/tumor.

Fig. 2(a) depicts the scanning electron microscope image of the MUTAB-coated AuNRs employed in this study. The choice of nanoparticle functionalization with MUTAB was adopted to promote cell uptake [33]. Tumors were ellipsoidal or quasi-spherical with an average dimension measured with a digital caliper along the longest axis of ~6.6 mm.

TABLE I
POSITIONS OF THE FBG SENSORS ALONG THE FIBER. THE POSITION CORRESPONDING TO THE CENTER OF EACH GRATING IS REPORTED (STARTING OF THE ARRAY EQUAL TO 0 mm)

Sensor	Distance along the fiber (mm)
FBG 1	0.25
FBG 2	1.45
FBG 3	2.65
FBG 4	3.85
FBG 5	5.05

B. Photothermal Experimental Set-Up and FBG-Based Thermometry

Prior to laser irradiation, mice were anesthetized with isoflurane (4% isoflurane in 1.5 L/min oxygen flow). Diode lasers (LuOcean Mini 4, Lumics, Berlin, Germany) with characteristic wavelengths of 940 nm and 1064 nm were used to irradiate the subcutaneous tumors. Lasers operated in a continuous mode at a power of 2.6 W and with a beam spot size chosen to cover the whole tumor regions (~0.8 cm in diameter). Laser radiation was delivered in contactless approach through a quartz optical fiber (OZ Optics Ltd., Ottawa, Canada), orthogonally positioned above subcutaneous tumors (Fig. 2(c)). FBG arrays, characterized by only a single connectorized end, were inserted into tumors through a 28.5-gauge needle, which was removed before the photothermal treatment; the central FBG sensor was located at the center of the tumor (Fig. 2(d)). Table I reports the FBG sensors positions along the optical fiber. The temperature profiles across the sensing part of the fiber were reconstructed from the measured spectra (sampling frequency equal to 10 Hz).

Once inserted inside the tumor, the sensors output before starting the thermal treatment was also acquired to assess the effect of physiological movements on the sensors response.

IV. Results and Discussion

A. Static and Dynamic Calibrations

The static temperature sensitivity coefficient S_t for the FBG array resulted equal to $(6.83 \pm 0.01) \cdot 10^{-6}$ °C^{-1}, which agrees with the typical static sensitivity of this kind of sensors.

Concerning the analysis of the FBG transient response, the estimated response time τ was 6.0 ± 1.2 ms. Fig. 3(a) reports the typical step response of one FBG sensor, while Fig. 3(b) depicts the trend of the natural logarithm of the error function and the fitting curve for the calculation of τ. The attained value of the time constant demonstrated the fast FBGs response, which may be well suited for application in which the detection of sudden temperature variations can be advantageous, such as in nanoparticle-enhanced photothermal ablation [34].

B. Effects of the Physiological Movement on the FBG Array Output Signal

Considering the strain sensitivity of FBGs, the employed sensors are prone to a cross-sensitivity phenomenon, ascribed

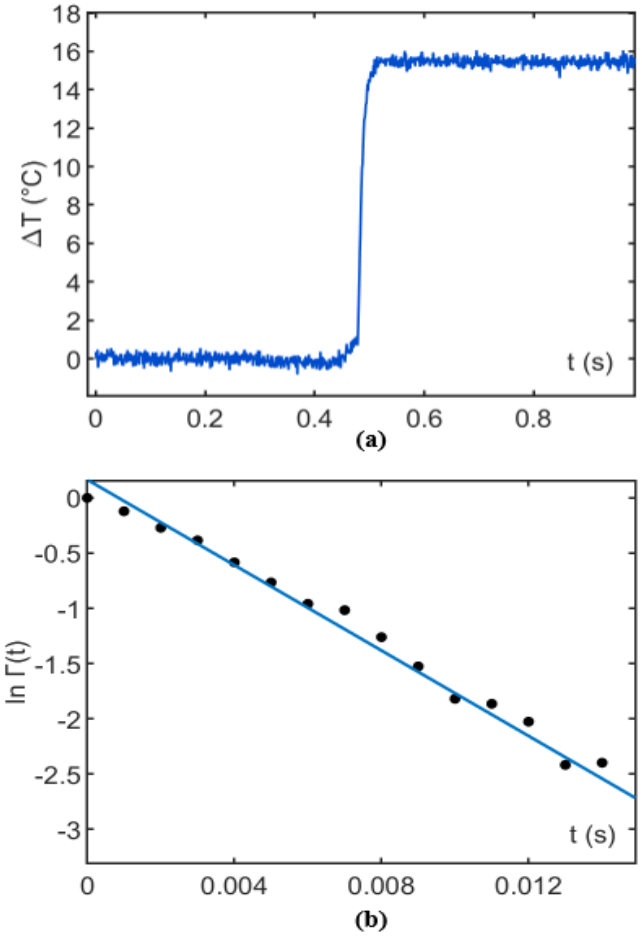

Fig. 3. (a) Step response of one of the 5 FBG sensors embedded in the employed optical fiber. (b) Trend of the natural logarithm of the error function versus time (4) and associated linear fitting curve for the estimation of the time constant.

to the deformation due to physiological movements of the animal, such as breathing, which may, in turn, influence the temperature monitoring [35]. Therefore, the FBGs output was acquired for 10 s before proceeding with the photothermal treatment to assess possible signal alterations due to physiological repetitive patterns (e.g., mouse respiratory rate: 60-220 breaths per minute [36]). The FBGs signals registered once the sensors were positioned within the subcutaneous tumors were compared with the optical signal acquired at environmental temperature (i.e., 20 °C) outside of the tumor. In both cases, the obtained root mean square errors (RMSEs) evaluated on the detected FBGs signals were lower than 0.23 °C. In Fig. 4, the output registered by the FBGs inserted within the tumor region prior to laser irradiation is reported.

Several studies estimated the measurement errors induced by respiratory movements on the FBG-based temperature monitoring of laser treatments both on *in vivo* large animal models and with simulated respiratory acts in the *ex vivo* scenario. The observed strain-induced artifacts resulted up to 2.5 °C - 3 °C, due to substantial fiber deformation [23], [35]. Conversely, in the present case study, the attained RMSE values suggest that the influence of the animal movements could be considered negligible on the registered temperature output.

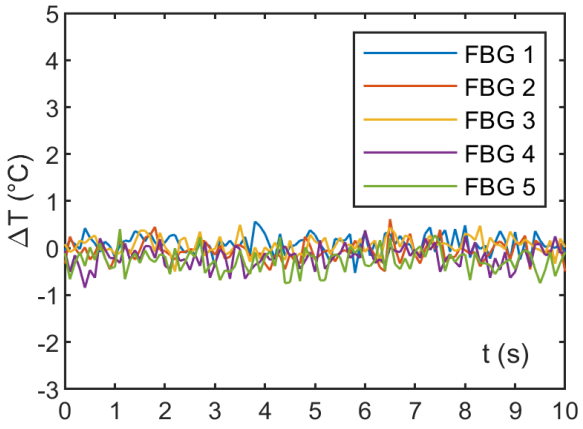

Fig. 4. Output signals (converted into temperature change versus time) of the FBG sensors positioned inside the subcutaneous tumor, before the laser irradiation procedure.

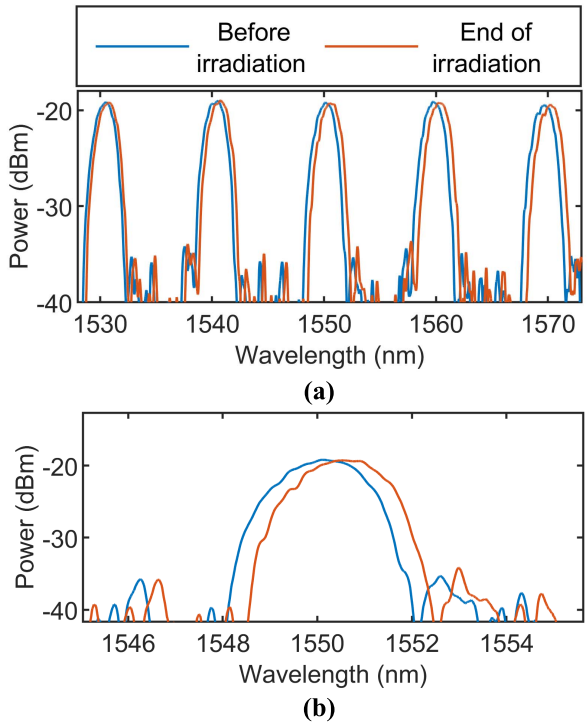

Fig. 5. (a) Reflection spectrum of the 5-FBG array fabricated with the femtosecond point-by-point writing technology before laser irradiation (blue line) and at the end of the exposure (red line). (b) Close-up on the optical spectrum relative to the central FBG of the array (FBG 3) recorded before and after NIR exposure.

C. High-Resolved Thermal Evaluation of in Vivo AuNR-Enhanced PTT in the Tumor Model

The signals acquired by the FBGs positioned within the subcutaneous tumors were analyzed in MATLAB®(Mathworks, Natick, MA, USA) environment. Fig. 5 shows a typical optical reflected spectrum before and at the end of the photothermal ablation procedure (Fig. 5(a)), with a focus on the central grating (FBG 3) (Fig. 5(b)).

Here, the wavelength variation due to the laser-induced temperature change can be observed. Indeed, the increment of temperature causes a proportional shift on the acquired

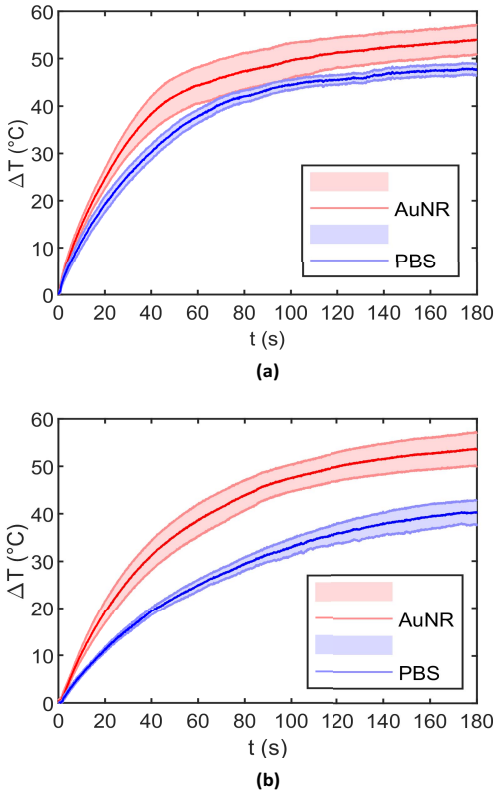

Fig. 6. Temperature evolution: mean temperature changes, and associated measurements uncertainties (shadowed lines), of tumors injected with AuNRs or PBS (saline solution) irradiated with laser at (a) 940 nm or (b) 1064 nm.

optical spectrum. In the present study, to reduce the possibility of cross-sensitivity to deformations, the FBG sensors were injected into tissue with a needle that was afterward removed prior to thermal treatment. That is to attain a slightly looser adhesion between the fiber and tissue, thus reducing possible strain effects, while preserving the multipoint measurement capability [37].

To characterize the thermal effect of the enhanced light-into-heat conversion, exerted by the laser-absorbing AuNRs, the evaluation of the internal temperature evolution of the tumor lesions was performed for the 4T1 tumor-bearing mice, injected with AuNRs or PBS, and subsequently undergoing laser irradiation at different wavelengths.

Fig. 6 represents the trends of the average temperature changes over time recorded by the FBG sensors during PTT for both AuNR-treated and PBS controls, and the associated measurement uncertainties (95% confidence level [38]).

Concerning the photothermal treatment performed with the diode laser emitting at 940 nm, the average temperature change among PBS-treated tumors was 47.6 ± 1.2 °C, while the combination of the laser-absorbing AuNRs resulted in an enhanced photothermal response which led to a temperature variation up to 53.9 ± 3.1 °C, after 3 min-laser exposure (Fig. 6(a)). Moreover, considering all PBS-injected tumors, the 940 nm laser showed the maximum temperature increase (i.e., 48.8 ± 1.0 °C). Conversely, the thermal treatment performed with the laser wavelength of 1064 nm, showed average temperature changes, after 3 min irradiation, equal to 40.0 ± 2.4 °C and 53.2 ± 3.4 °C, in the absence and after intratumoral administration of AuNRs, respectively (Fig. 6(b)). The subcutaneous breast cancer tissue, on which the experimental trials have been performed, is a dynamic and highly complex turbid media, in which the light propagation and subsequent photothermal conversion are regulated by the intrinsic tissue optical and physical properties [39]. Despite the difficulty to estimate the optical properties of the specific samples, our attained FBG-based temperature measurements in PBS controls are in accordance with the optical properties calculated for the skin and breast tissue [40], [41]. The obtained higher temperatures changes in PBS-injected tumors for the radiation of 940 nm may be ascribed to the higher tissue absorption close to 940 nm, compared to 1064 nm (e.g., effective attenuation coefficients of 3.1 cm^{-1} and 2.5 cm^{-1} for wavelengths of 950 nm and 1064 nm, respectively, calculated for the skin in a small animal model [40]). Moreover, the 940 nm stimulation wavelength is closer to the absorption peak of lipids, which are one of the principal components of breast tissue [42], [43]. The injection of AuNRs resulted in higher temperature values registered by the FOSs in all the nanoparticle-treated groups. Particularly, the mean temperature difference between AuNR and control groups after an exposure time of 3 min was ∼13 °C in the case of 1064 nm, and ∼6 °C for 940 nm-radiation. These temperature results suggest that with 1064 nm laser irradiation associated with AuNRs a higher therapy selectivity may be achieved compared to the AuNR-laser radiation combination at 940 nm wavelength. The different temperature increase after administration of the nanoparticles can be explained by the different penetration depths characterizing the employed lasers. While the 940 nm light is mostly absorbed by the superficial components of tissue due to reduced optical penetration, the 1064 nm lasers can further penetrate the biological media, thus reaching also AuNRs located in the inner part of the lesion, where the FBGs are placed. The subsequent photothermal conversion might explain the highest thermal values compared to controls, for the latter case. It is worth noticing that in case of AuNR injections, in all the treated groups, the measurement uncertainties of the registered temperature resulted higher than in control cases. This is in line with studies concerning the difficulty to regulate the effective photothermal outcome due to the complicated control of nanoparticle distribution at the tumor site [31]. That, in turn, may lead to different temperature values registered by the sensors of the FBG array, embedded within the same subcutaneous tumors.

The thermal efficiency ratio expressed as the average temperature increase of the tumor group undergoing AuNR-assisted photothermal ablation with respect to the average temperature change experienced by the PBS tumors undergoing laser irradiation resulted equal to 1.25 and 1.33, respectively for 940 nm, and 1064 nm wavelengths. The obtained values are consistent with the result attained in a previous study for the investigation of the internal tumor temperature on subcutaneous tumors (∼1.36), considering the same AuNR concentration, same exposure time, with different temperature monitoring techniques, i.e., k-type thermocouples [4]. The described differences can be due to the employed setting parameters and wavelength, as well as nanoparticle size utilized in [4].

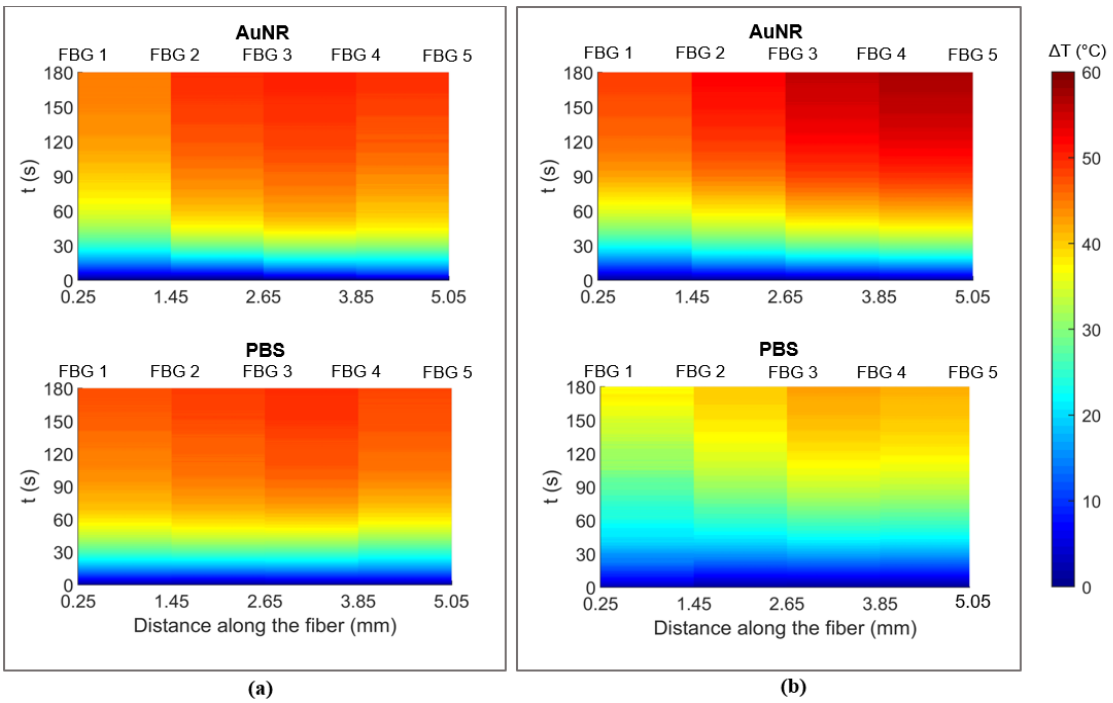

Fig. 7. Two-dimensional thermal maps (distance along the fiber versus time) attained through FBG-based thermometry of AuNR- or PBS-injected subcutaneous tumors undergoing irradiation at: (a) 940 nm, or (b) 1064 nm laser wavelength.

Regarding the evaluation of the thermal distribution, the reduced dimensions (0.5 mm grating length) of the adopted point-by-point laser-inscribed FBGs, compared to the ones used for thermometry during thermal treatments (with a typical minimal grating length of 1 mm [20], [21], [44]), resulted in a high spatial resolution, i.e., 1.2 mm. This feature permitted to reconstruct high spatially resolved two-dimensional thermal maps of the internal tumor temperature during the photothermal procedure, in tumors with an average dimension of ∼6.6 mm.

Fig. 7 shows the average temperature values in time for each FBG, distributed along the array, during PTT performed on AuNRs- and PBS-injected tumors performed at the different radiation wavelengths. A linear interpolation was applied between consecutive FBG sensors. For all the temperature change profiles an increment is observable after the application of laser radiation at the instant $t = 0$ s. In case of AuNRs assistance for the two different wavelengths and also PBS samples for 940 nm, temperature changes >45 °C are observable in tumors after 2 min-exposure times; whereas, when the PBS was injected, temperature increases remained lower than 43 °C for 1064 nm radiations, even at the end of treatment.

The acquired temperatures are predominantly in accordance with the relative position of FBG sensors and the Gaussian intensity distribution of the forward peaked laser beam, since in ∼70% of tumors the highest temperature was measured by the central sensor of each array (FBG 3) positioned along the beam axis, hence subjected to a relevant temperature gradient.

The lack of this correspondence in some samples can be due to the intrinsic biological tissue optical inhomogeneities [45], and to the non-uniform nanoparticle distribution [9] in case of AuNR-assisted PTT. These factors can lead to maximum temperature values registered by FBGs which are not located along the beam central axis, thus more distant from the laser tip.

Overall, the millimeter-resolved FBG-based thermometry proved to be effective for the accurate description of the tumor thermal behavior during the laser treatments. Considering the strict criteria required for an adequate temperature monitoring of thermal therapies, i.e., spatial resolution of 1-2 mm, acquisition time of seconds, recommended accuracy of 1-2 °C [46], [47], the implemented sensing system demonstrated to meet the desired characteristics. Indeed, the sensing solution based on femtosecond laser inscribed FBG array (spatial resolution of 1.2 mm, accuracy of 0.1 °C) allowed for the detection of thermal gradients occurring during nanoparticle-assisted PTT performed on tumors with an average dimension of ∼6.6 mm. The interesting features, such as sub-centimetric dimensions, multiplexing capability, and flexibility [13] encourage the use of these sensors as minimally invasive multipoint temperature probes in neoplasms with small sizes or complex geometries. Furthermore, the capability to assess the internal temperature evolution in several points with high temporal resolution can be beneficial during procedures in which fast heating kinetics are expected.

The sensing solution herein proposed permitted to assess the internal temperature increase during treatments, and the attainment of two-dimensional maps of tissue thermal effect, due to the laser-nanoparticle interaction, thanks to highly accurate and resolved measurements. The immunity from electromagnetic interferences, biocompatibility, and high metrological

characteristics (e.g., short time response, high thermal sensitivity, and sub-millimetric resolution) are also advantageous features of the implemented FBG-based sensing system for nanoparticle-enhanced PTTs. Furthermore, the possibility to embed several FBGs within a single fiber to be inserted within deep-seated tissue reduced the invasiveness of the thermometry approach compared to contact and single-point measurement transducers, often utilized in nanoparticle-assisted PTT [4], [8], [48]. For instance, the number of inserting points should be increased to attain the same multipoint temperature description in the tumor by means of thermocouples. Additionally, the use of FBGs sensors permitted the avoidance of overestimation or underestimation of the obtained temperature change due to heat conductivity and radiation absorption, which are typical downsides of thermocouples [49], [50], thanks to the NIR radiation-compatible properties of silica glass and polyimide material [16], [29], [51] of the fiber.

To the best of our knowledge, this is the first-ever detailed investigation of the use of custom-made FBG arrays for the monitoring of *in vivo* nanoparticle-enhanced PTT in breast cancer tumor models. In this context, future studies could benefit from an increased number of gratings within the same fiber or distributed fiber optic-based sensors which theoretically permit an infinite number of sensing points. This could allow the investigation of the optimal thermal effect in diverse relevant positions within the tumor region, during nanoparticle-mediated PTT. Additionally, thanks to the fast response and accuracy of the sensing system, further developments should focus on the real-time analysis of the achieved internal temperature during the irradiation and the subsequent adjustment of the procedural settings. This could in turn pave the way to more controlled thermal dosimetry for nanoparticle-assisted thermal treatments.

V. Conclusion

In the present study, we investigated the feasibility of FBG arrays for internal tumor thermometry during *in vivo* AuNR-mediated PTT in breast cancer models. The FBG sensors, obtained with femtosecond laser inscription, allowed for high spatial resolution and multiple sub-millimetric sensing points within a single fiber. The metrological characteristics of the sensors fulfilled the requirements for temperature monitoring during thermal therapy applications. Moreover, the investigation of the effects of the physiological movements demonstrated that the output of the sensors was not influenced by the strain cross-sensitivity. Concerning the PTT, this quasi-distributed sensing solution allowed the comparison of the temperature enhancement induced by different combinations of AuNRs and laser wavelengths (i.e., 940 nm and 1064 nm). The results of this study pave the way to an alternative approach for multipoint temperature measurements inside tumors undergoing PTT, as a support for the definition of the optimal therapy settings.

VI. Acknowledgment

This project has received funding from the European Research Council (ERC) under the European Union's Horizon 2020 research and innovation programme (Grant agreement No. 759159).

References

[1] M. Malvezzi *et al.*, "European cancer mortality predictions for the year 2019 with focus on breast cancer," *Ann. Oncol.*, vol. 30, no. 5, pp. 781–787, May 2019, doi: 10.1093/annonc/mdz051.

[2] *Conquering Cancer Mission Possible*, Eur. Commission, Luxembourg City, Luxembourg, 2020.

[3] A. Ashkbar, F. Rezaei, F. Attari, and S. Ashkevarian, "Treatment of breast cancer *in vivo* by dual photodynamic and photothermal approaches with the aid of curcumin photosensitizer and magnetic nanoparticles," *Sci. Rep.*, vol. 10, no. 1, Dec. 2020, Art. no. 21206, doi: 10.1038/s41598-020-78241-1.

[4] R. Mooney, E. Schena, P. Saccomandi, A. Zhumkhawala, K. Aboody, and J. M. Berlin, "Gold nanorod-mediated near-infrared laser ablation: *In vivo* experiments on mice and theoretical analysis at different settings," *Int. J. Hyperthermia*, vol. 33, no. 2, pp. 150–159, Feb. 2017, doi: 10.1080/02656736.2016.1230682.

[5] S. Asadi, L. Bianchi, M. De Landro, S. Korganbayev, E. Schena, and P. Saccomandi, "Laser-induced optothermal response of gold nanoparticles: From a physical viewpoint to cancer treatment application," *J. Biophoton.*, vol. 14, no. 2, Feb. 2021, Art. no. e202000161, doi: 10.1002/jbio.202000161.

[6] I. Maor *et al.*, "Laser-induced thermal response and controlled release of copper oxide nanoparticles from multifunctional polymeric nanocarriers," *Sci. Technol. Adv. Mater.*, vol. 22, no. 1, pp. 218–233, Dec. 2021, doi: 10.1080/14686996.2021.1883406.

[7] S. Thomsen, "Pathologic analysis of photothermal and photomechanical effects of laser-tissue interactions," *Photochem. Photobiol.*, vol. 53, no. 6, pp. 825–835, Jun. 1991, doi: 10.1111/j.1751-1097.1991.tb09897.x.

[8] E. B. Dickerson *et al.*, "Gold nanorod assisted near-infrared plasmonic photothermal therapy (PPTT) of squamous cell carcinoma in mice," *Cancer Lett.*, vol. 269, no. 1, pp. 57–66, Sep. 2008, doi: 10.1016/j.canlet.2008.04.026.

[9] R. Mooney, E. Schena, A. Zhumkhawala, K. S. Aboody, and J. M. Berlin, "Internal temperature increase during photothermal tumour ablation in mice using gold nanorods," in *Proc. 37th Annu. Int. Conf. IEEE Eng. Med. Biol. Soc. (EMBC)*, Aug. 2015, pp. 2563–2566, doi: 10.1109/EMBC.2015.7318915.

[10] A. Farashahi *et al.*, "Real-time mapping of heat generation and distribution in a laser irradiated agar phantom loaded with gold nanoparticles using MR temperature imaging," *Photodiagnosis Photodyn. Therapy*, vol. 25, pp. 66–73, Mar. 2019, doi: 10.1016/j.pdpdt.2018.11.010.

[11] X. Meng *et al.*, "Accurate and real-time temperature monitoring during MR imaging guided PTT," *Nano Lett.*, vol. 20, no. 4, pp. 2522–2529, Apr. 2020, doi: 10.1021/acs.nanolett.9b05267.

[12] K. T. V. Grattan and B. T. Meggit, *Optical Fiber Sensor Technology Advanced Applications—Bragg Gratings and Distributed Sensors*. Dordrecht, The Netherlands: Kluwer, 2000.

[13] F. Morra *et al.*, "Spatially resolved thermometry during laser ablation in tissues: Distributed and quasi-distributed fiber optic-based sensing," *Opt. Fiber Technol.*, vol. 58, Sep. 2020, Art. no. 102295, doi: 10.1016/j.yofte.2020.102295.

[14] S. Korganbayev, M. De Landro, F. Morra, A. Cigada, and P. Saccomandi, "Fiber optic sensors for distributed and quasi-distributed temperature measurement," in *Proc. IEEE SENSORS*, Oct. 2020, pp. 1–4, doi: 10.1109/SENSORS47125.2020.9278937.

[15] D. Tosi, "Review and analysis of peak tracking techniques for fiber Bragg grating sensors," *Sensors*, vol. 17, no. 10, p. 2368, Oct. 2017, doi: 10.3390/s17102368.

[16] A. V. Dostovalov, A. A. Wolf, A. V. Parygin, V. E. Zyubin, and S. A. Babin, "Femtosecond point-by-point inscription of Bragg gratings by drawing a coated fiber through ferrule," *Opt. Exp.*, vol. 24, no. 15, p. 16232, Jul. 2016, doi: 10.1364/OE.24.016232.

[17] Q. Yu, Y. Zhang, Y. Dong, Y. P. Li, C. Wang, and H. Chen, "Study on optical fiber Bragg grating temperature sensors for human body temperature monitoring," in *Proc. Symp. Photon. Optoelectron. (SOPO)*, May 2012, pp. 1–4, doi: 10.1109/SOPO.2012.6271111.

[18] S. Ambastha, S. Pant, S. Umesh, V. Vazhayil, and S. Asokan, "Feasibility study on thermography of embedded tumor using fiber Bragg grating thermal sensor," *IEEE Sensors J.*, vol. 20, no. 5, pp. 2452–2459, Mar. 2020, doi: 10.1109/JSEN.2019.2950973.

[19] R. Correia, S. James, S.-W. Lee, S. P. Morgan, and S. Korposh, "Biomedical application of optical fibre sensors," *J. Opt.*, vol. 20, no. 7, Jul. 2018, Art. no. 073003, doi: 10.1088/2040-8986/aac68d.

[20] G. Palumbo *et al.*, "Temperature profile of *ex-vivo* organs during radio frequency thermal ablation by fiber Bragg gratings," *J. Biomed. Opt.*, vol. 21, no. 11, Nov. 2016, Art. no. 117003, doi: 10.1117/1.jbo.21.11.117003.

[21] P. Saccomandi *et al.*, "Theoretical analysis and experimental evaluation of laser-induced interstitial thermotherapy in *ex vivo* porcine pancreas," *IEEE Trans. Biomed. Eng.*, vol. 59, no. 10, pp. 2958–2964, Oct. 2012, doi: 10.1109/TBME.2012.2210895.
[22] R. Gassino, Y. Liu, M. Konstantaki, A. Vallan, S. Pissadakis, and G. Perrone, "A fiber optic probe for tumor laser ablation with integrated temperature measurement capability," *J. Lightw. Technol.*, vol. 35, no. 16, pp. 3447–3454, Aug. 15, 2017, doi: 10.1109/JLT.2016.2618618.
[23] D. Polito *et al.*, "A needlelike probe for temperature monitoring during laser ablation based on fiber Bragg grating: Manufacturing and characterization," *J. Med. Devices*, vol. 9, no. 4, pp. 1–28, Dec. 2015, doi: 10.1115/1.4030624.
[24] L. Bianchi *et al.*, "Fiber Bragg grating sensors for thermometry during gold nanorods-mediated photothermal therapy in tumor model," in *Proc. IEEE SENSORS*, Oct. 2020, pp. 1–4, doi: 10.1109/SENSORS47125.2020.9278580.
[25] T. Erdogan, "Fiber grating spectra," *J. Lightw. Technol.*, vol. 15, no. 8, pp. 1277–1294, 1997, doi: 10.1109/50.618322.
[26] A. Othonos, K. Kalli, D. Pureur, and A. Mugnier, "Fibre Bragg gratings," in *Wavelength Filters in Fibre Optics*. Berlin, Germany: Springer, 2006, pp. 189–269.
[27] C. R. Liao and D. N. Wang, "Review of femtosecond laser fabricated fiber Bragg gratings for high temperature sensing," *Photon. Sensors*, vol. 3, no. 2, pp. 97–101, Jun. 2013, doi: 10.1007/s13320-012-0060-9.
[28] S. J. Mihailov *et al.*, "Bragg grating writing through the polyimide coating of high NA optical fibres with femtosecond IR radiation," *Opt. Commun.*, vol. 281, no. 21, pp. 5344–5348, Nov. 2008, doi: 10.1016/j.optcom.2008.07.056.
[29] L. Huang, R. S. Dyer, R. J. Lago, A. A. Stolov, and J. Li, "Mechanical properties of polyimide coated optical fibers at elevated temperatures," *Proc. SPIE*, vol. 9702, Mar. 2016, Art. no. 97020Y, doi: 10.1117/12.2210957.
[30] S. Korganbayev *et al.*, "Closed-loop temperature control based on fiber Bragg grating sensors for laser ablation of hepatic tissue," *Sensors*, vol. 20, no. 22, p. 6496, Nov. 2020, doi: 10.3390/s20226496.
[31] R. Mooney *et al.*, "Neural stem cell-mediated intratumoral delivery of gold nanorods improves photothermal therapy," *ACS Nano*, vol. 8, no. 12, pp. 12450–12460, Dec. 2014, doi: 10.1021/nn505147w.
[32] R. S. Figliola and D. E. Beasley, *Theory and Design for Mechanical Measurements*, 2nd ed. New York, NY, USA: Wiley, 1995, doi: 10.1080/03043799508928292.
[33] K. Schnarr *et al.*, "Gold nanoparticle-loaded neural stem cells for photothermal ablation of cancer," *Adv. Healthcare Mater.*, vol. 2, no. 7, pp. 976–982, Jul. 2013, doi: 10.1002/adhm.201300003.
[34] B. Jang, Y. S. Kim, and Y. Choi, "Effects of gold nanorod concentration on the depth-related temperature increase during hyperthermic ablation," *Small*, vol. 7, no. 2, pp. 265–270, Jan. 2011, doi: 10.1002/smll.201001532.
[35] C. Cavaiola *et al.*, "Error of a temperature probe for cancer ablation monitoring caused by respiratory movements: *Ex vivo* and *in vivo* analysis," *IEEE Sensors J.*, vol. 16, no. 15, pp. 5934–5941, Aug. 2016, doi: 10.1109/JSEN.2016.2574959.
[36] J. E. Harkness, P. V. Turner, S. VandeWoude, and C. L. Wheler, *Harkness and Wagner's Biology and Medicine of Rabbits and Rodents*, 5th ed. Ames, IA, USA: Wiley, 2010.
[37] B. A. Patterson, D. D. Sampson, P. A. Krug, and S. K. Jones, "*In vivo* quasi-distributed temperature sensing with fibre Bragg gratings," in *Conf. Lasers Electro-Opt. Postconf. Tech. Dig.*, 2001, pp. 402–403, doi: 10.1109/CLEO.2001.947973.
[38] *Evaluation of Measurement Data—Guide to the Expression of Uncertainty in Measurement*, JCGM, Int. Org. Standardization, Geneva, Switzerland, 2008.
[39] F. Asllanaj, S. Contassot-Vivier, A. Hohmann, and A. Kienle, "Light propagation in biological tissue," *J. Quant. Spectrosc. Radiat. Transf.*, vol. 224, pp. 78–90, Feb. 2019, doi: 10.1016/j.jqsrt.2018.11.001.
[40] W. F. Cheong, S. A. Prahl, and A. J. Welch, "A review of the optical properties of biological tissues," *IEEE J. Quantum Electron.*, vol. 26, no. 12, pp. 2166–2185, Dec. 1990. [Online]. Available: https://omlc.org/~prahl/pubs/pdfx/cheong90a.pdf, doi: 10.1109/3.64354.
[41] P. Taroni, A. Pifferi, A. Torricelli, and R. Cubeddu, "Time-resolved optical spectroscopy and imaging of breast," *Opto-Electron. Rev.*, vol. 12, no. 2, pp. 249–253, 2004.
[42] P. Taroni *et al.*, "Non-invasive optical estimate of tissue composition to differentiate malignant from benign breast lesions: A pilot study," *Sci. Rep.*, vol. 7, no. 1, Feb. 2017, Art. no. 40683, doi: 10.1038/srep40683.
[43] P. Taroni, A. Bassi, D. Comelli, A. Farina, R. Cubeddu, and A. Pifferi, "Diffuse optical spectroscopy of breast tissue extended to 1100 nm," *J. Biomed. Opt.*, vol. 14, no. 5, 2009, Art. no. 054030, doi: 10.1117/1.3251051.
[44] P. Saccomandi, E. Schena, M. Diana, F. M. Di Matteo, G. Costamagna, and J. Marescaux, "Multipoint temperature monitoring in liver undergoing computed tomography-guided radiofrequency ablation with fiber Bragg grating probes," in *Proc. 38th Annu. Int. Conf. IEEE Eng. Med. Biol. Soc. (EMBC)*, Aug. 2016, pp. 5174–5179, doi: 10.1109/EMBC.2016.7591893.
[45] V. L. Weber, "Detection of inhomogeneities in biological tissues by the methods of confocal microscopy," *Radiophys. Quantum Electron.*, vol. 41, no. 5, pp. 417–427, May 1998, doi: 10.1007/BF02676569.
[46] L. Frich, "Non-invasive thermometry for monitoring hepatic radiofrequency ablation," *Minimally Invasive Therapy Allied Technol.*, vol. 15, no. 1, pp. 18–25, Jan. 2006, doi: 10.1080/13645700500470025.
[47] M. A. Lewis, R. M. Staruch, and R. Chopra, "Thermometry and ablation monitoring with ultrasound," *Int. J. Hyperthermia*, vol. 31, no. 2, pp. 163–181, Feb. 2015, doi: 10.3109/02656736.2015.1009180.
[48] G. P. Goodrich, L. Bao, K. Gill-Sharp, K. L. Sang, J. Wang, and J. D. Payne, "Photothermal therapy in a murine colon cancer model using near-infrared absorbing gold nanorods," *J. Biomed. Opt.*, vol. 15, no. 1, 2010, Art. no. 018001, doi: 10.1117/1.3290817.
[49] P. Saccomandi, E. Schena, and S. Silvestri, "Techniques for temperature monitoring during laser-induced thermotherapy: An overview," *Int. J. Hyperthermia*, vol. 29, no. 7, pp. 609–619, Nov. 2013, doi: 10.3109/02656736.2013.832411.
[50] F. Manns, P. J. Milne, X. Gonzalez-Cirre, D. B. Denham, J.-M. Parel, and D. S. Robinson, "*In situ* temperature measurements with thermocouple probes during laser interstitial thermotherapy (LITT): Quantification and correction of a measurement artifact," *Lasers Surg. Med. Off. J. Amer. Soc. Laser Med. Surg.*, vol. 23, no. 2, pp. 94–103, 1998.
[51] K. Weir, "Optical fiber sensor technology," *J. Mod. Opt.*, vol. 42, no. 4, p. 938, Apr. 1995, doi: 10.1080/713824421.

Leonardo Bianchi (Graduate Student Member, IEEE) received the M.Sc. *(cum laude)* degree in biomedical engineering from the Politecnico di Milano in 2019, where he is currently pursuing the Ph.D. degree with the Department of Mechanical Engineering. He is working in the framework of the European Research Council (ERC)-funded LASER OPTIMAL project (Laser Ablation: SElectivity and monitoRing for OPTImal tuMor removAL), Politecnico di Milano. His research interests include optimization of tumor laser ablation, from both the numerical modeling and experimental assessment, nanoparticle-assisted photothermal therapies, and the related sensing techniques for temperature monitoring during treatments.

Rachael Mooney received the Ph.D. degree in biochemistry from the University of Colorado at Boulder in 2009. She is currently an Assistant Research Professor with the Department of Developmental and Stem Cell Biology, City of Hope Comprehensive Cancer Center, and the Beckman Research Institute, Duarte, CA, USA. Her research interests include cell therapy, drug delivery, biomaterials, nanotechnology, oncolytic viruses, immunology, and translational studies. Her honors include the 2005 Top 10 Young Investigators Award (Wound Healing Society), and Postdoctoral Fellowships awarded by the California Institute of Regenerative Medicine in 2010 and Ladies Auxiliary of the Veterans of Foreign Wars in 2013.

Yvonne Cornejo received the B.S. degree in animal science from California Polytechnic University, Pomona, CA, USA, in 2005, the D.V.M. degree from the College of Veterinary Medicine, Western University of Health Sciences, Pomona, in 2015, and the Ph.D. degree in biological sciences from the City of Hope Irell & Manella Graduate School in 2020. She is currently a Laboratory Animal Veterinarian with Valley Biosystems. Her research interests include nanoparticle technology, oncolytic viruses, translational studies, and comparative medicine. Her awards include a Supplemental Diversity Award for an RO1.

Caitlyn Hyde received the bachelor's degree in bioenvironmental sciences from Texas A&M University in 2019. She was a Research Associate I with the Department of Developmental and Stem Cell Biology, City of Hope Comprehensive Cancer Center, and the Beckman Research Institute, Duarte, CA, USA.

Emiliano Schena (Senior Member, IEEE) received the Ph.D. degree in biomedical engineering from the Università Campus Bio-Medico di Roma in 2009. He is currently an Associate Professor with the Università Campus Bio-Medico di Roma. His main research interests include systems for monitoring physiological parameters, application of fiber optic sensors in medicine, and laser ablation for cancer removal.

Jacob M. Berlin received the B.A. *(magna cum laude)* degree in chemistry from Harvard University in 2001, and the Ph.D. degree in organometallic chemistry from CalTech in 2006. He studied with Nobel Laureate Bob Grubbs, CalTech. He completed Postdoctoral Training with MIT and Rice University focusing on synthetic chemistry and nanotechnology. From 2010 to 2019, he was a Professor with the City of Hope. He is currently the CEO of Terray Therapeutics, a VC-backed biotechnology company pioneering next generation drug discovery and development. His honors and awards include being named one of the Rising Stars and Young Nanoarchitects in Materials Science by the Royal Society of Chemistry and the STOP CANCER Research Career Development Award.

Karen Aboody received the medical degree from the New York's Mount Sinai School of Medicine. She received training at the Harvard Medical School. Since 2013, she has been a Professor with the Department of Neurosciences and Division of Neurosurgery, City of Hope National Medical Center, and the Beckman Research Institute, Duarte, CA, USA. She is a member of the American Association for Cancer Research, American Society of Gene & Cell Therapy, and others. She is at the forefront of research into using neural stem cells to assist in the delivery of chemotherapy to brain tumors.

Paola Saccomandi (Senior Member, IEEE) received the Ph.D. degree in biomedical engineering from the Università Campus Bio-Medico di Roma in 2014. From 2016 to 2018, she was a Postdoctoral Researcher with the IHU - Institute of Image-Guided Surgery of Strasbourg. Since 2018, she has been an Associate Professor with the Department of Mechanical Engineering, Politecnico di Milano. She is the Principal Investigator of the European Research Council grant LASER OPTIMAL. Her main research interests include fiber optic sensors, biomedical imaging, and the development of light-based approaches for hyperthermal tumor treatment and monitoring.